

Supplemental Materials

Molecular Biology of the Cell

Zhu et al.

SUPPLEMENTAL MATERIALS

Molecular Biology of the Cell

Zhu et al.

SUPPLEMENTAL MOVIE LEGEND

MOVIE 1: *ync13Δ* cells lyse during or after cell separation. Time lapse fluorescence microscopy (UltraVIEW Vox CSUX1 system; PerkinElmer) of wt (top) and *ync13Δ* (bottom) cells expressing Rlc1-tdTomato as the contractile ring marker. Images of Rlc1 (left) and DIC (right) are shown. Interval, 1 min. Photobleaching during image acquisition was not corrected. This video corresponds to Figure 2C. Display rate is 8 fps. Bar, 5 μm.

MOVIE 2: Plasma membrane closure in *ync13Δ* cells. Wt (left) and *ync13Δ* (right) cells expressing GFP-Psy1 (green) and Rlc1-tdTomato (magenta) are shown. Interval, 1 min. This video corresponds to Figure S4B. Display rate is 8 fps. Bar, 5 μm.

MOVIE 3: Calcofluor staining of *ync13Δ* cells during cytokinesis. Calcofluor stained wt (left) and *ync13Δ* (right) cells were imaged in time lapse microscopy with 1 min interval. The video corresponds to Figure 2F. Display rate is 8 fps.

MOVIE 4: Localization of glucan synthases Bgs1, Bgs4, and Ags1 in *ync13Δ* cells during cytokinesis. Wt (left) and *ync13Δ* (right) cells expressing both GFP tagged glucan synthases (green) and Rlc1-tdTomato (magenta) are shown. Interval, 1 min. This video corresponds to Figure 4, A-C. Display rate is 8 fps. Bar, 5 μm.

MOVIE 5: Vesicle tracking in *ync13-19 sec8-1* cells during septum maturation. GFP-Syb1 was used as a vesicle marker for tracking vesicle movement in representative cells in continuous 2 min time-lapse movies. Tracked vesicle movements are shown in colored lines. We recorded the location of the vesicles in each frame and connected these locations to visualize the tracks of vesicles. The vesicles are present at or near the leading end of the tracks in each frame until they were delivered to the division plane. Time in min : sec. This video corresponds to Figure 5D. Display rate is 8 fps. Bar, 5 μm.

MOVIE 6: Vesicle tracking in *ync13Δ* cells during septum maturation. mEGFP-Ypt3 was used as a vesicle marker for tracking vesicle movement in representative wt (left) and *ync13Δ* (right) cells in continuous 2 min time-lapse movies. Tracked vesicle movements are shown in colored lines as in Movie 5. Time in min : sec. This video corresponds to Figure 6G. Display rate is 8 fps.

MOVIE 7: Visualization of endocytic patches in *ync13Δ* cells. Wt (left) and *ync13Δ* (right) cells expressing Fim1-mEGFP Rlc1-tdTomato were used in the 2 min continuous time-lapse movie in green channel. Representative cells during septum maturation are shown. Time in min : sec. This video corresponds to Figure 7, B and C. Display rate is 8 fps.

SUPPLEMENTAL TABLE S1: *S. pombe* strains used in this study.

Strain	Genotype	Figure/Table/Movie/ Reference
JW5664	<i>h⁻ ync13-mECitrine-kanMX6 ade6-210 ura4-D18 leu1-32</i>	Fig 1, B, E, and F
JW5969	<i>sad1-mCherry-natMX6 ync13-mECitrine-kanMX6 ade6-M210 leu1-32 ura4-D18</i>	Fig 1C
JW5814	<i>ync13-mECitrine-kanMX6 rlc1-mCherry-natMX6 ade6-210 leu1-32 ura4-D18</i>	Fig 1D
JW6657	<i>h⁻ ync13-mMaple3-kanMX6 ade6-210 leu1-32 ura4-D18</i>	Fig 1F
JW5664	<i>h⁻ ync13-mECitrine-kanMX6 ade6-210 ura4-D18 leu1-32</i>	Fig S1, B and D-G; S2, B-E
JW6207	<i>h⁻ ync13-3YFP-hphMX6 ade6-210 leu1-32 ura4-D18</i>	Fig S1C
JW5689	<i>ync13-mECitrine-kanMX6 cdc15-140 ade6-210 leu1-32 ura4-D18</i>	Fig S1F
JW5967	<i>its3-1 ync13-mECitrine-kanMX6 ade6-210 leu1-32 ura4-D18</i>	Fig S1G
JW5984	<i>h⁻ kanMX6-Pync13-mECitrine-ync13(591-1237) ade6-M216 leu1-32 ura4-D18</i>	Fig S2, A-E
JW5985	<i>h⁻ ync13(1-1013)-mECitrine-kanMX6 ade6-M216 leu1-32 ura4-D18</i>	Fig S2, A-E
JW5986	<i>h⁻ ync13(1-804)-mECitrine-kanMX6 ade6-M216 leu1-32 ura4-D18</i>	Fig S2, A-E
JW5987	<i>h⁻ ync13(1-590)-mECitrine-kanMX6 ade6-M216 leu1-32 ura4-D18</i>	Fig S2, A-E
JW5861	<i>ync13Δ::kanMX6 rlc1-tdTomato-natMX6 ade6 leu1-32 ura4-D18</i>	Fig S2A
JW4008	<i>h⁻ nod1-mECitrine-kanMX6 ade6-M210 leu1-32 ura4-D18</i>	Fig S2D
JW4912	<i>Pgef2-mECitrine-4Gly-gef2 ade6 leu1-32 ura4-D18</i>	Fig S2D
JW3952	<i>h⁻ rng8-mECitrine-kanMX6 ade6-M210 leu1-32 ura4-D18</i>	Fig S2D
JW4946	<i>h⁻ rng9-mECitrine-kanMX6 ade6-M210 leu1-32 ura4-D18</i>	Fig S2D
JW81	<i>h⁻ ade6-210 ura4-D18 leu1-32</i>	Fig S2, A and D
YZ3-2	<i>ync13⁺/ync13Δ::kanMX6 rlc1-tdTomato/rlc1-tdTomato ade6-210/ade6-216 leu1-32/leu1-32 ura4-D18/ura4-D18</i>	Fig 2, A and B
JW5861	<i>ync13Δ::kanMX6 rlc1-tdTomato-natMX6 ade6 leu1-32 ura4-D18</i>	Fig 2, C and F-H; S4A
JW1341	<i>h⁻ rlc1-tdTomato-natMX6 ade6-M210 leu1-32 ura4-D18</i>	Fig 2C; S4A
JW3313	<i>h⁻ kanMX6-3nmt1-mEGFP rlc1-tdTomato-natMX6 ade6-M210 leu1-32 ura4-D18</i>	Fig 2, D and E
JW5983	<i>ync13Δ::kanMX6 kanMX6-3nmt1-mEGFP rlc1-tdTomato-natMX6 ade6 leu1-32 ura4-D18</i>	Fig 2, D and E
JW81	<i>h⁻ ade6-210 leu1-32 ura4-D18</i>	Fig 3, F-H
JW2402	<i>h⁻ psy1Δ::kanMX6 leu1⁺::GFP-psy1 rlc1-tdTomato-natMX6 ade6-M210 ura4</i>	Fig S4B
JW6723	<i>ync13Δ::kanMX6 psy1Δ::kanMX6 leu1⁺::GFP-psy1 rlc1-tdTomato-natMX6 ade6 ura4</i>	Fig S4B
JW5862	<i>ync13-4-his5⁺-kanMX6 ade6-M210 leu1-32 ura4</i>	Fig 3A
PPG6840	<i>h⁻ rho1-596-natMX6 leu1-32 ura4-D18</i>	Fig 3A

JW5971	<i>ync13Δ::kanMX6 rlc1-tdTomato-natMX6 ade6 leu1-32 ura4-D18+ pUR19-Rho1</i>	Fig 3B
JW5972	<i>ync13Δ::kanMX6 rlc1-tdTomato-natMX6 ade6 leu1-32 ura4-D18+ pUR19</i>	Fig 3B
JW2245	<i>h⁺ rgf3-mECitrine-kanMX6 ade6-M210 leu1-32 ura4-D18</i>	Fig 3C
JW6544	<i>h⁻ rgf3-mECitrine-kanMX6 ync13Δ::kanMX6 ade6 leu1-32 ura4-D18</i>	Fig 3C
JW1170	<i>h⁺ pck2-mYFP-kanMX6 ade6-M210 leu1-32 ura4-D18</i>	Fig 3D
JW6065	<i>ync13Δ::kanMX6 pck2-mYFP-kanMX6 ade6 leu1-32 ura4-D18</i>	Fig 3D
JW5593	<i>h⁻ leu1::kanMX6-P3nmt1-pkc1(HR1-C2)-mECitrine ade6-M210 leu1-32 ura4-D18</i>	Fig 3E
JW6004	<i>ync13Δ::kanMX6 leu1::kanMX6-P3nmt1-pkc1(HR1-C2)-mECitrine ade6 leu1-32 ura4-D18</i>	Fig 3E
JW5664	<i>h⁻ ync13-mECitrine-kanMX6 ade6-210 leu1-32 ura4-D18</i>	Fig 3F
JW5928	<i>h⁺ rho1-596-natMX6 ync13-mECitrine-kanMX6 ade6-210 leu1-32 ura4-D18</i>	Fig 3F
JW5249	<i>GFP-bgs1-leu1⁺ bgs1Δ::ura4⁺ rlc1-tdTomato-natMX6 ade6-M210 leu1-32 ura4-D18</i>	Fig 4, A and D; S4E
JW6616	<i>GFP-bgs1-leu1⁺ bgs1Δ::ura4⁺ rlc1-tdTomato-natMX6 ync13Δ::kanMX6 ade6 ura4-D18</i>	Fig 4, A and D; S4E
JW6153	<i>bgs4Δ::ura4⁺ Pbgs4⁺::GFP-bgs4⁺-leu1⁺ rlc1-tdTomato-natMX6 leu1-32 ura4-D18</i>	Fig 4, B and D; S4E
JW6152	<i>bgs4Δ::ura4⁺ Pbgs4⁺::GFP-bgs4⁺-leu1⁺ rlc1-tdTomato-natMX6 ync13Δ::kanMX6 ade6 his3-D1 leu1-32 ura4-D18</i>	Fig 4, B and D; S4E
JW6808	<i>rlc1-tdTomato-natMX6 ags1Δ 3'UTR_{ags1+}::ags1⁺-GFP:leu1⁺:ura4⁺ ync13Δ::kanMX6 ade6 leu1-32 ura4-D18</i>	Fig 4, C and D; S4E
JW6810	<i>rlc1-tdTomato-natMX6 ags1Δ 3'UTR_{ags1+}::ags1⁺-GFP:leu1⁺:ura4⁺ade6 leu1-32 ura4-D18</i>	Fig 4, C and D; S4E
JW6747	<i>ync13Δ::kanMX6 eng1-GFP-kan^R rlc1-tdTomato-natMX6 ade6 leu1-32 ura4-D18</i>	Fig 4E
JW6748	<i>eng1-GFP-kan^R rlc1-tdTomato-natMX6 ade6 leu1-32 ura4-D18</i>	Fig 4E
JW81	<i>h⁻ ade6-210 ura4-D18 leu1-32</i>	Fig S4, C-F
JW5862	<i>ync13-4-his5⁺-kanMX6 ade6-M210 leu1-32 ura4</i>	Fig S4, C and D
JW1696	<i>h⁺ bgs1-191 ade6-M210 leu1-32 ura4-D18</i>	Fig S4D
JW6778	<i>ync13-4-his5⁺-kanMX6 bgs1-191 ade6-M210 leu1-32 ura4</i>	Fig S4D
JW7551	<i>cwgl-2 ade6-M210 leu1-32 ura4</i>	Fig S4D
JW7549	<i>ync13-4-his5⁺-kanMX6 cwgl-2 ade6-M210 leu1-32 ura4</i>	Fig S4D
JW7577	<i>h⁻ mok1-664 ync13-4-his5⁺-kanMX6 leu1</i>	Fig S4D
DH664	<i>h⁻ leu1 mok1-664</i>	Fig S4D; Katayama, <i>et al.</i> , 1999
JW5861	<i>ync13Δ::kanMX6 rlc1-tdTomato-natMX6 ade6 leu1-32 ura4-D18</i>	Fig S4F
JW2319	<i>h⁺ eng1Δ::kanMX4 ade6 leu1-32 ura4-D18</i>	Fig S4F
JW6745	<i>ync13Δ::kanMX6 eng1Δ::kanMX4 rlc1-tdTomato-natMX6 ade6 leu1-32 ura4-D18</i>	Fig S4F
JW81	<i>h⁻ ade6-210 ura4-D18 leu1-32</i>	Fig 5A; S5B, and S6A

JW5862	<i>ync13-4-his5⁺-kanMX6 ade6-M210 leu1-32 ura4</i>	Fig 5A; S6A
JW3915	<i>h⁺ sec8-1 leu1-32 ura4-D18</i>	Fig 5A; S5B
JW5931	<i>sec8-1 ync13-4-his5⁺-kanMX6 ade6 leu1-32 ura4-D18</i>	Fig 5A
JW5249	<i>GFP-bgs1-leu1⁺ bgs1Δ::ura4⁺ rlc1-tdTomato-natMX6 ade6-M210 leu1-32 ura4-D18</i>	Fig 5B
JW7294	<i>sec8-1 GFP-bgs1-leu1⁺ bgs1Δ::ura4⁺ rlc1-tdTomato-natMX6 ade6-M210 leu1-32 ura4-D18</i>	Fig 5B
JW5911	<i>h⁺ ync13-4-his5⁺-kanMX6 GFP-bgs1-leu1⁺ bgs1Δ::ura4⁺ rlc1-tdTomato-natMX6 ade6-M210 leu1-32 ura4</i>	Fig 5B
JW7516	<i>sec8-1 ync13-4-his5⁺-kanMX6 GFP-bgs1-leu1⁺ bgs1Δ::ura4⁺ rlc1-tdTomato-natMX6 ade6-M210 leu1-32 ura4</i>	Fig 5B
JW6550	<i>h⁻ GFP-syb1-kanMX6 ade6 leu1-32 ura4-D18</i>	Fig 5, C and D
JW7339	<i>ync13-19-his5⁺-kanMX6 sec8-1 GFP-syb1-kanMX6 ade6 leu1-32 ura4</i>	Fig 5, C and D
JW7341	<i>ync13-19-his5⁺-kanMX6 GFP-syb1-kanMX6 ade6 leu1-32 ura4</i>	Fig 5, C and D
JW6549	<i>sec8-1 GFP-syb1-kanMX6 ade6 leu1-32 ura4-D18</i>	Fig 5, C and D
JW5861	<i>ync13Δ::kanMX6 rlc1-tdTomato-natMX6 ade6 leu1-32 ura4-D18</i>	Fig S5, A-C
JW2716	<i>h⁺ exo70Δ::kanMX4 ade6 leu1-32 ura4-D18</i>	Fig S6A
JW5929	<i>exo70Δ::kanMX4 ync13-4-his5⁺-kanMX6 ade6 leu1-32 ura4-D18</i>	Fig S6A
JW7062	<i>sec3-GFP-kanMX6 rlc1-tdTomato-natMX6 ade6 leu1-32 ura4-D18</i>	Fig S6B
JW7066	<i>sec3-GFP-kanMX6 rlc1-tdTomato-natMX6 ync13Δ::kanMX6 ade6 leu1-32 ura4-D18</i>	Fig S6B
JW7061	<i>h⁻ sec8-GFP-ura4⁺ rlc1-tdTomato-natMX6 leu1-32 ura4-D18</i>	Fig S6B
JW7065	<i>sec8-GFP-ura4⁺ rlc1-tdTomato-natMX6 ync13Δ::kanMX6 leu1-32 ura4-D18</i>	Fig S6B
JW7320	<i>trs120-3GFP-kanMX6 rlc1-tdTomato-natMX6 ade6 leu1-32 ura4-D18</i>	Fig 6A
JW7318	<i>ync13Δ::kanMX6 trs120-3GFP-kanMX6 rlc1-tdTomato-natMX6 ade6 leu1-32 ura4-D18</i>	Fig 6A
JW6208	<i>ync13Δ::kanMX6 GFP-syb1-kanMX6 rlc1-tdTomato-natMX6 ade6 leu1-32</i>	Fig 6B
JW6548	<i>h⁺ GFP-syb1-kanMX6 rlc1-tdTomato-natMX6 ade6 leu1-32 ura4-D18</i>	Fig 6B
JW7356	<i>kanMX6-Pypt3-mEGFP-ypt3 rlc1-tdTomato-natMX6 ade6 leu1-32 ura4-D18</i>	Fig 6, C-G; S6C
JW7357	<i>kanMX6-Pypt3-mEGFP-ypt3 rlc1-tdTomato-natMX6 ync13Δ::kanMX6 ade6 leu1-32 ura4-D18</i>	Fig 6, C-G; S6C
JW7056	<i>h⁻ rlc1-tdTomato-natMX6 fim1-mEGFP-kanMX6 ade6 leu1-32 ura4-D18</i>	Fig 7, A-D
JW7057	<i>fim1-mEGFP-kanMX6 rlc1-tdTomato-natMX6 ync13Δ::kanMX6 ade6 leu1-32 ura4-D18</i>	Fig 7, A-D
JW7191	<i>ede1-mGFP-kanMX6 rlc1-tdTomato-natMX6 ync13Δ::kanMX6 ade6 leu1-32 ura4-D18</i>	Fig 7, E and F
JW7194	<i>ede1-mGFP-kanMX6 rlc1-tdTomato-natMX6 ade6 leu1-32 ura4-D18</i>	Fig 7, E and F
JW7193	<i>pan1-mGFP-kanMX6 rlc1-tdTomato-natMX6 ade6 leu1-32 ura4-D18</i>	Fig S6D
JW7190	<i>pan1-mGFP-kanMX6 rlc1-tdTomato-natMX6 ync13Δ::kanMX6 ade6 leu1-32 ura4-D18</i>	Fig S6D

JW7192	<i>end4-mGFP-kanMX6 rlc1-tdTomato-natMX6 ade6 leu1-32 ura4-D18</i>	Fig S6D
JW7189	<i>end4-mGFP-kanMX6 rlc1-tdTomato-natMX6 ync13Δ::kanMX6 ade6 leu1-32 ura4-D18</i>	Fig S6D
JW5861	<i>ync13Δ::kanMX6 rlc1-tdTomato-natMX6 ade6 leu1-32 ura4-D18</i>	Movies 1 and 3
JW1341	<i>h⁻ rlc1-tdTomato-natMX6 ade6-M210 leu1-32 ura4-D18</i>	Movie 1
JW2402	<i>h⁻ rlc1-tdTomato-natMX6 psy1Δ::kanMX6 leu1⁺::GFP-psy1 ade6-M210 ura4</i>	Movie 2
JW6723	<i>ync13Δ::kanMX6 rlc1-tdTomato-natMX6 psy1Δ::kanMX6 leu1⁺::GFP-psy1 ade6 ura4</i>	Movie 2
JW81	<i>h⁻ ade6-210 ura4-D18 leu1-32</i>	Movie 3
JW5249	<i>GFP-bgs1-leu1⁺ bgs1Δ::ura4⁺ rlc1-tdTomato-natMX6 ade6-M210 leu1-32 ura4-D18</i>	Movie 4
JW6616	<i>GFP-bgs1-leu1⁺ bgs1Δ::ura4⁺ rlc1-tdTomato-natMX6 ync13Δ::kanMX6 ade6 ura4-D18</i>	Movie 4
JW6153	<i>bgs4Δ::ura4⁺ Pbgs4⁺::GFP-bgs4⁺-leu1⁺ rlc1-tdTomato-natMX6 leu1-32 ura4-D18</i>	Movie 4
JW6152	<i>bgs4Δ::ura4⁺ Pbgs4⁺::GFP-bgs4⁺-leu1⁺ rlc1-tdTomato-natMX6 ync13Δ::kanMX6 leu1-32 ura4-D18 his3-D1 ade6</i>	Movie 4
JW6808	<i>ync13Δ::kanMX6 rlc1-tdTomato-natMX6 ags1Δ 3'UTRags1⁺::ags1⁺-GFP:leu1⁺:ura4⁺ade6 leu1-32 ura4-D18</i>	Movie 4
JW6810	<i>rlc1-tdTomato-natMX6 ags1Δ 3'UTRags1⁺::ags1⁺-GFP:leu1⁺:ura4⁺ade6 leu1-32 ura4-D18</i>	Movie 4
JW6550	<i>h⁻ GFP-syb1-kanMX6 ade6 leu1-32 ura4-D18</i>	Movie 5
JW7339	<i>ync13-19-his5⁺-kanMX6 sec8-1 GFP-syb1-kanMX6 ade6 leu1-32 ura4</i>	Movie 5
JW7341	<i>ync13-19-his5⁺-kanMX6 GFP-syb1-kanMX6 ade6 leu1-32 ura4</i>	Movie 5
JW6549	<i>sec8-1 GFP-syb1-kanMX6 ade6 leu1-32 ura4-D18</i>	Movie 5
JW7356	<i>kanMX6-Pypt3-mEGFP-ypt3 rlc1-tdTomato-natMX6 ade6 leu1-32 ura4-D18</i>	Movie 6
JW7357	<i>kanMX6-Pypt3-mEGFP-ypt3 rlc1-tdTomato-natMX6 ync13Δ::kanMX6 ade6 leu1-32 ura4-D18</i>	Movie 6
JW7056	<i>h⁻ rlc1-tdTomato-natMX6 fim1-mEGFP-kanMX6 ade6 leu1-32 ura4-D18</i>	Movie 7
JW7057	<i>rlc1-tdTomato-natMX6 fim1-mEGFP-kanMX6 ync13Δ::kanMX6 ade6 leu1-32 ura4-D18</i>	Movie 7
JW5862	<i>ync13-4-his5⁺-kanMX6 ade6-M210 leu1-32 ura4</i>	Table 1
JW5888	<i>myo2-E1 ync13-4-his5⁺-kanMX6 ade6 leu1-32 ura4</i>	Table 1
JW2252	<i>myo2-E1 ade6 leu1-32 ura4-D18</i>	Table 1
JW5887	<i>cdc15-140 ync13-4-his5⁺-kanMX6 ade6-M210 leu1-32 ura4</i>	Table 1
JW1743	<i>cdc15-140 ade6-M210 leu1-32 ura4-D18</i>	Table 1
JD141	<i>h⁻ imp2Δ::ura4⁺ ade6-M216 leu1-32 ura4-D18</i>	Table 1; Demeter and Sazor, 1998
PPG6840	<i>h⁻ rho1-596-natMX6 leu1-32 ura4-D18</i>	Table 1; Viana <i>et al.</i> , , 2013
JW3563	<i>h⁻ art1Δ::kanMX6 ade6-210 leu1-32 ura4-D18</i>	Table 1
JW4028	<i>h⁻ rga7Δ::kanMX6 ade6-M210 leu1-32 ura4-D18</i>	Table 1

JW3039	<i>h⁺ pck1Δ::kanMX4 ade6 leu1-32 ura4-D18</i>	Table 1
JW5996	<i>pck2-Δ1::kanMX6 ync13-4-his5⁺-kanMX6 ade6 leu1-32 ura4-D18</i>	Table 1
JW376	<i>h⁺ pck2-Δ1::kanMX6 ade6 leu1-32 ura4-D18</i>	Table 1
IJ767	<i>h⁻ sec3-913-hphMX6 ade6-M216 leu1-32 ura4-D18</i>	Table 1; Jourdain, <i>et al.</i> , 2012
JW6517	<i>sec3-913-hphMX6 ync13-4-his5⁺-kanMX6 ade6 leu1-32 ura4</i>	Table 1
IJ1032	<i>h⁻ sec3-916-hphMX6 ade6-M216 leu1-32 ura4-D18</i>	Table 1; Jourdain, <i>et al.</i> , 2012
JW6519	<i>sec3-916-hphMX6 ync13-4-his5⁺-kanMX6 ade6 leu1-32 ura4</i>	Table 1
JW6002	<i>h⁻ rho3Δ::natMX6 ade6-210 leu1-32 ura4-D18</i>	Table 1
JW6515	<i>h⁻ rho3Δ::natMX6 ync13-4-his5⁺-kanMX6 ade6-210 leu1-32 ura4</i>	Table 1
JW828	<i>h⁻ for3Δ::kanMX6 ade6 leu1-32 ura4-D18</i>	Table 1
JW6779	<i>ync13-19-his5⁺-kanMX6 ade6-M210 leu1-32 ura4</i>	Table 1
JW8355	<i>for3Δ::kanMX6 ync13-19-his5⁺-kanMX6 ade6 leu1-32 ura4-D18</i>	Table 1
JW7036	<i>h⁻ trs120-ts1-his5⁺-kanMX6 his5Δ ade6-M210 leu1-32 ura4</i>	Table 1
JW7383	<i>ync13-4-his5⁺-kanMX6 trs120-ts1-his5⁺-kanMX6 ade6-M210 leu1-32 ura4</i>	Table 1
VS845	<i>h⁺ end4Δ::kanMX6 ade6-M210 leu1-32 ura4-D18 his3-D1</i>	Table 1; V. Sirotkin
JW7526	<i>h⁻ ync13-4-his5⁺-kanMX6 end4Δ::kanMX6 ade6 leu1-32 ura4 his3-D1</i>	Table 1
VS822	<i>h⁺ pan1ΔACV::kanMX6 ade6-M210 leu1-32 ura4-D18 his3-D1</i>	Table 1; V. Sirotkin
JW7524	<i>h⁺ ync13-4-his5⁺-kanMX6 pan1ΔACV::kanMX6 ade6-M210 leu1-32 ura4</i>	Table 1
JW1696	<i>h⁺ bgs1-191 ade6-M210 leu1-32 ura4-D18</i>	Table 1
JW6778	<i>ync13-4-his5⁺-kanMX6 bgs1-191 ade6-M210 leu1-32 ura4</i>	Table 1
JW7551	<i>cwg1-2 ade6-M210 leu1-32 ura4</i>	Table 1
JW7549	<i>ync13-4-his5⁺-kanMX6 cwg1-2 ade6-M210 leu1-32 ura4</i>	Table 1
JW7577	<i>h⁻ mok1-664 ync13-4-his5⁺-kanMX6 leu1</i>	Table 1
DH664	<i>h⁻ mok1-664 leu1</i>	Table 1; Katayama, <i>et al.</i> , 1999
JW2244	<i>h⁺ fic1Δ::kanMX4 ade6 leu1-32 ura4-D18</i>	Table 1
JW6617	<i>h⁺ fic1Δ::kanMX4 ync13-4-his5⁺-kanMX6 ade6 leu1-32 ura4</i>	Table 1
JW2640	<i>h⁺ pxl1Δ::kanMX4 ade6 leu1-32 ura4-D18</i>	Table 1
JW6622	<i>h⁺ pxl1Δ::kanMX4 ync13-4-his5⁺-kanMX6 ade6 leu1-32 ura4</i>	Table 1
JW6060	<i>h⁻ rho2Δ::hphMX6 ade6-210 leu1-32 ura4-D18</i>	Table 1
JW6116	<i>ync13-4-his5⁺-kanMX6 rho2Δ::hphMX6 ade6-M210 leu1-32 ura4-D18</i>	Table 1
JW3915	<i>h⁺ sec8-1 leu1-32 ura4-D18</i>	Table 1

JW5931	<i>sec8-1 ync13-4-his5⁺-kanMX6 ade6 leu1-32 ura4-D18</i>	Table 1
JW7340	<i>sec8-1 ync13-19-his5⁺-kanMX6 ade6 leu1-32 ura4</i>	Table 1
JW2716	<i>h⁺ exo70Δ::kanMX4 ade6 leu1-32 ura4-D18</i>	Table 1
JW5929	<i>exo70Δ::kanMX4 ync13-4-his5⁺-kanMX6 ade6 leu1-32 ura4-D18</i>	Table 1
212	<i>h⁺ myo52Δ::ura4⁺ ade6-M210 leu1-32 ura4-D18</i>	Table 1; Win et al., 2001
JW6818	<i>ync13-4-his5⁺-kanMX6 myo52Δ::ura4⁺ ade6-M210 leu1-32 ura4</i>	Table 1
JW144	<i>h⁺ fim1-Δ1::kanMX6 ade6 leu1-32 ura4-D18</i>	Table 1
JW6710	<i>ync13-4-his5⁺-kanMX6 fim1-Δ1::kanMX6 ade6 leu1-32 ura4</i>	Table 1
JW1234	<i>h⁺ arp2-1 mam2::leu2 ade6 leu1-32 ura4-D18</i>	Table 1
JW6683	<i>ync13-4-his5⁺-kanMX6 arp2-1 mam2::LEU2 ade6 leu1-32 ura4</i>	Table 1
JW1319	<i>h⁺ acp2Δ::kanMX6 his7-366 ade6-M210 leu1-32 ura4-D18</i>	Table 1
JW6682	<i>ync13-4-his5⁺-kanMX6 acp2Δ::kanMX6 ade6-210 leu1-32 ura4</i>	Table 1
JW1240	<i>h⁺ wsp1Δ::kanMX6 ade6-M216 leu1-32 ura4-D18 his3-D1</i>	Table 1
JW6684	<i>ync13-4-his5⁺-kanMX6 wsp1Δ::kanMX6 ade6 leu1-32 ura4-D18 his3-D1</i>	Table 1
JW2319	<i>h⁺ eng1Δ::kanMX4 ade6 leu1-32 ura4-D18</i>	Table 1
JW6654	<i>eng1Δ::kanMX4 ync13-4-his5⁺-kanMX6 ade6 leu1-32 ura4</i>	Table 1
JW2318	<i>h⁺ agn1Δ::kanMX4 ade6 leu1-32 ura4-D18</i>	Table 1
JW6653	<i>h⁺ agn1Δ::kanMX4 ync13-4-his5⁺-kanMX6 ade6 leu1-32 ura4</i>	Table 1
JW1256	<i>h⁻ its3-1 leu1-32</i>	Table 1
JW5968	<i>h⁻ its3-1 ync13-4-his5⁺-kanMX6 leu1-32</i>	Table 1
YSM836	<i>h⁺ cdc42-1625(A158V)-kanMX leu1-32 ura4-D18</i>	Table 1; Martin et al., 2007
PPG15.41	<i>h⁻ rho4Δ::kanMX6 leu1-32 ura4-D18</i>	Table 1; Santos et al., 2005
JW6514	<i>rho4Δ::kanMX6 ync13-4-his5⁺-kanMX6 ade6 leu1-32 ura4</i>	Table 1
JW6066	<i>ync13Δ::kanMX6 ade6 leu1-32 ura4-D18</i>	Table 1
KGY2030	<i>h⁻ rgf3(lad1-1) ade6-M210 leu1-32 ura4-D18</i>	Table 1; Morrell-Falvey et al., 2005
JW6547	<i>rgf3(lad1-1) ync13Δ::kanMX6 ade6 leu1-32 ura4-D18</i>	Table 1
JW6745	<i>ync13Δ::kanMX6 eng1Δ::kanMX4 rlc1-tdTomato-natMX6 ade6 leu1-32 ura4-D18</i>	Table 1
JW6746	<i>ync13Δ::kanMX6 agn1Δ::kanMX4 ade6 leu1-32 ura4-D18</i>	Table 1

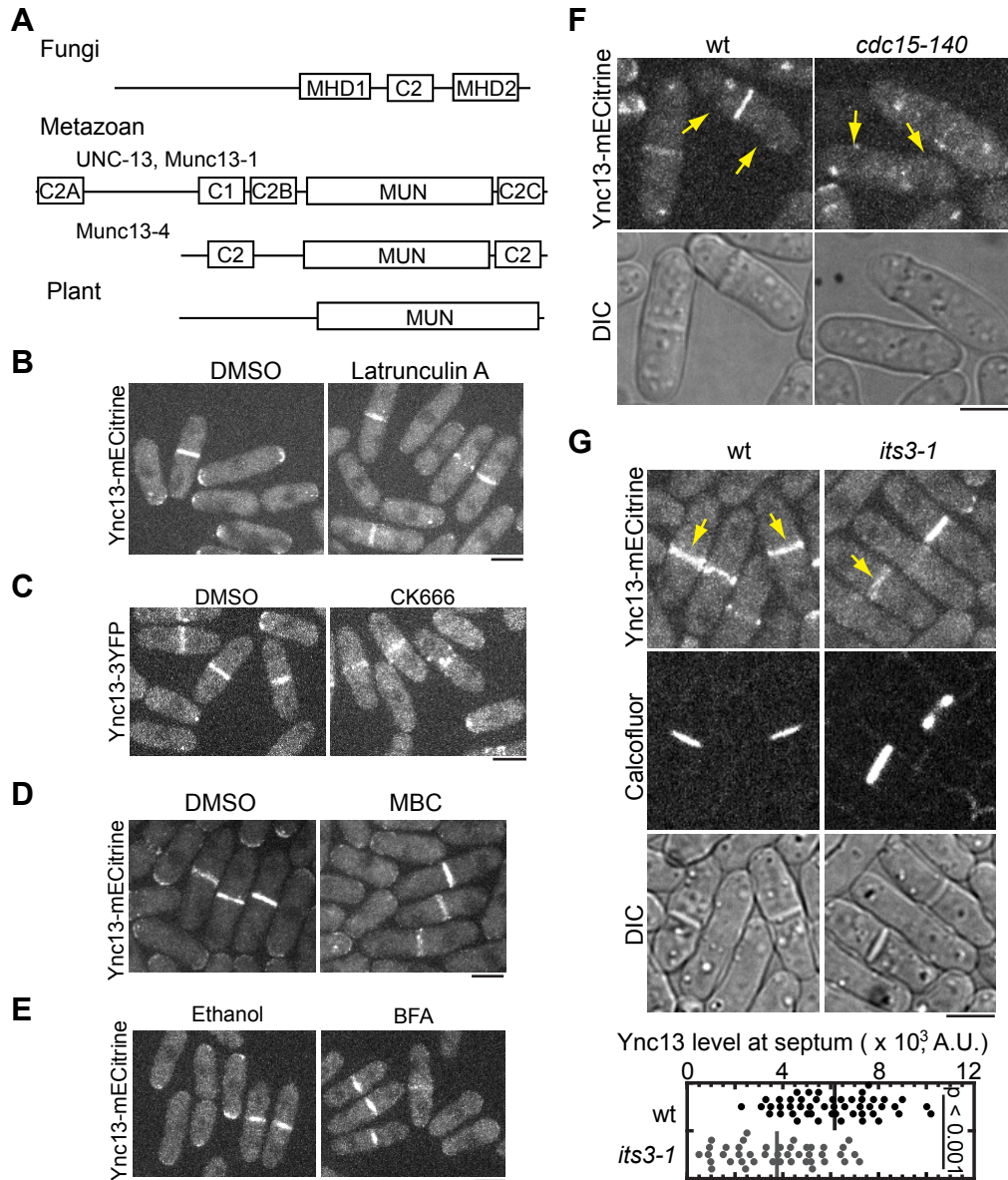


FIGURE S1: Ync13 depends on the cues from the contractile ring and plasma membrane lipids for localization. (A) Comparisons of domain organizations of UNC-13/Munc13 family proteins. The domain organization of fungal, mammalian (UNC-13, Munc13-1, and Munc13-4), and plant proteins are shown. (B-E) Ync13 localization is independent of actin, microtubule, or membrane trafficking. Cells were treated with Latrunculin A (B), Arp2/3 complex inhibitor CK666 (C), MBC (D), or BFA (E) before imaging. (F, G) Localization of Ync13 depends on F-BAR protein Cdc15 (F) and Its3 (G). Cells were grown at 25°C and shifted to 36°C for 2 h and imaged at 36°C (F) or grown and imaged at 25°C (G). Arrows in (F) point out examples of nuclear locations for cells in anaphase B. Arrows in (G) mark Ync13 localization during septum maturation (indicated by Calcofluor staining), which was quantified. Bars, 5 μ m.

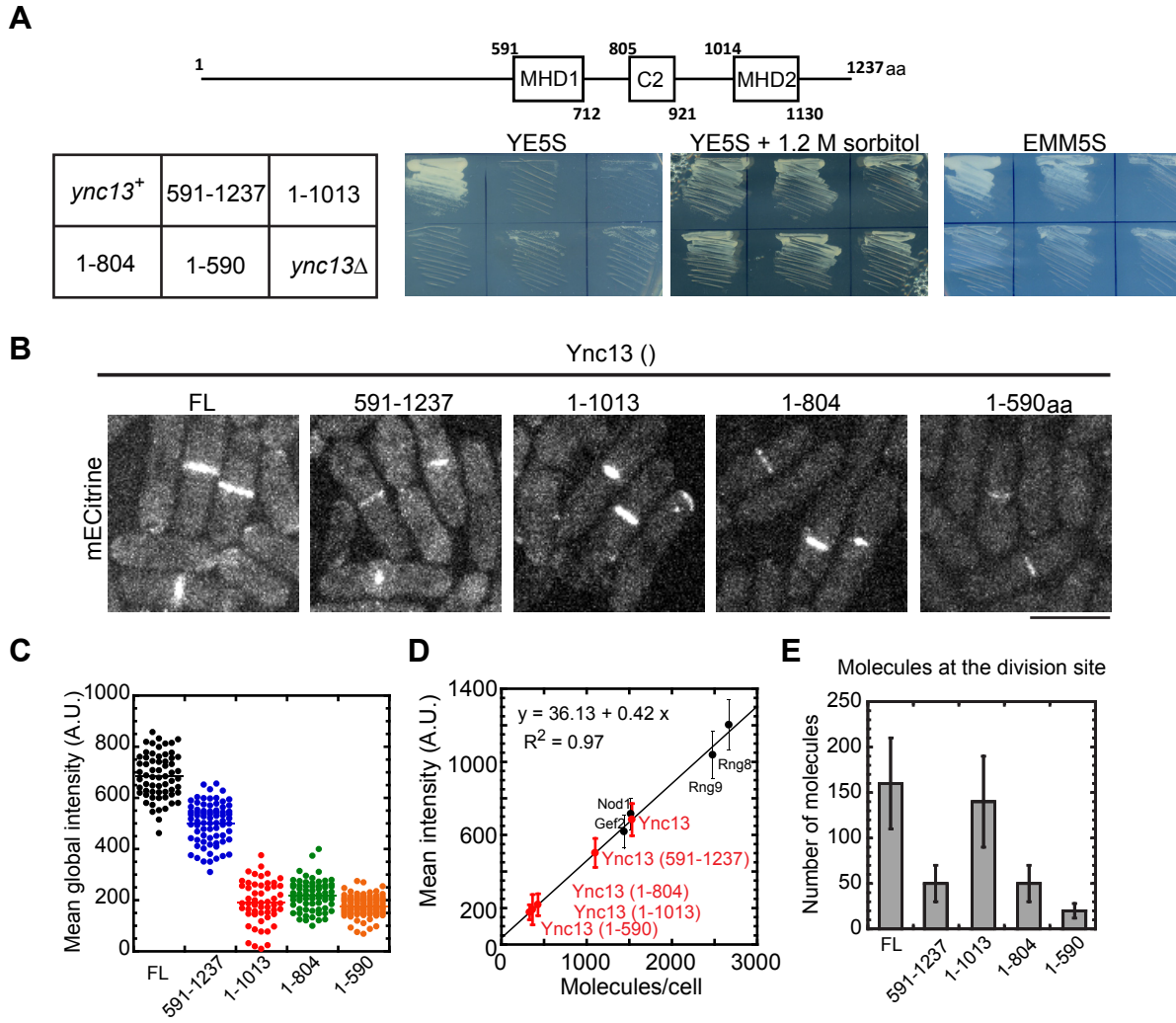


FIGURE S2: Domain analyses of Ync13. (A) Schematics of Ync13 and growth test of strains expressing Ync13 truncations. Ync13 truncations constructed are lethal on YE5S, but viable on YE5S + 1.2 M sorbitol and EMM5S medium. Cells were grown on YE5S for 2 d or on EMM5S for 3 d at 25°C. (B) Localization of Ync13 truncations. (C, D) Global mean intensity of Ync13 FL or truncations were quantified (C) and plotted to the standard curve of proteins with known molecule numbers (D). (E) Local molecule numbers of Ync13 and truncations at the division site obtained using the standard curve in (D). Bar, 5 μ m.

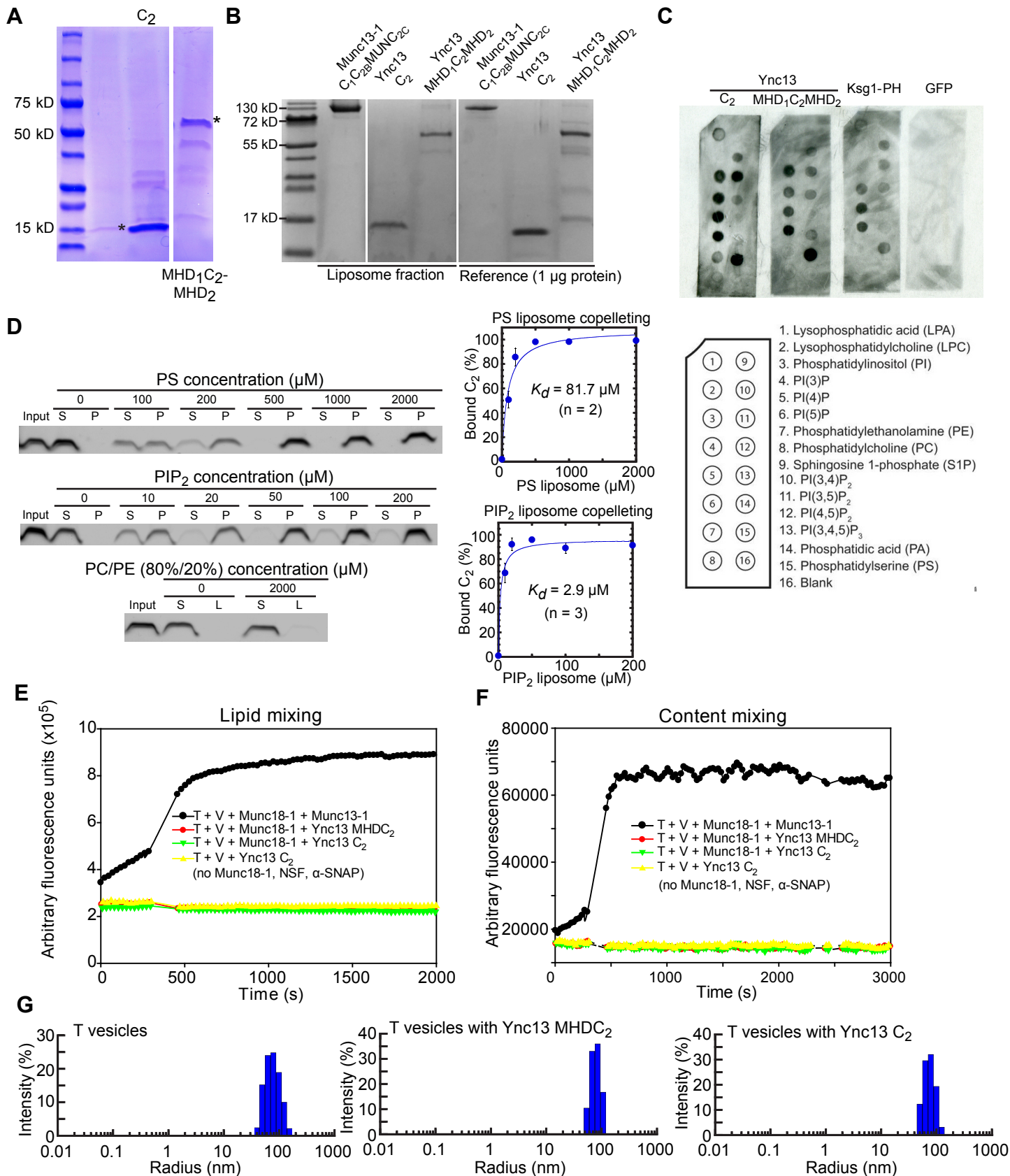


FIGURE S3: Ync13 interacts with lipids but does not promote vesicle fusion. (A) Coomassie blue staining of purified 6His tagged Ync13 C₂ domain and MHD₁C₂MHD₂ fragment. (B) Ync13 C₂ and MHD₁C₂MHD₂ fragments co-float with T-liposomes. Lipid bound fraction after ultracentrifugation and 1 μg of each input protein were loaded. Munc13-1 is a positive control. (C) Protein-lipid overlay assays for purified 6His-Ync13(C₂) and 6His-Ync13(MHD₁C₂MHD₂). 6His-Ksg1(PH) is a positive control and 6His-GFP is a negative control. Lipids on the membrane are listed at the bottom. (D) Ync13 C₂ domain interacts with various concentrations of PS and PIP₂ but not PC/PE in liposome copelleting assays (see Materials and methods). The *K_d* of C₂ domain with PS or PIP₂ liposomes is shown. (E, F) Lipid mixing (E) and content mixing (F) assays with purified Ync13 fragments in (A). T liposomes (T) and V liposomes (V) were incubated with the indicated proteins plus NSF and α-SNAP unless indicated otherwise. (G) Ync13 C₂ and MHD₁C₂MHD₂ do not cluster membrane in dynamic light scattering assays.

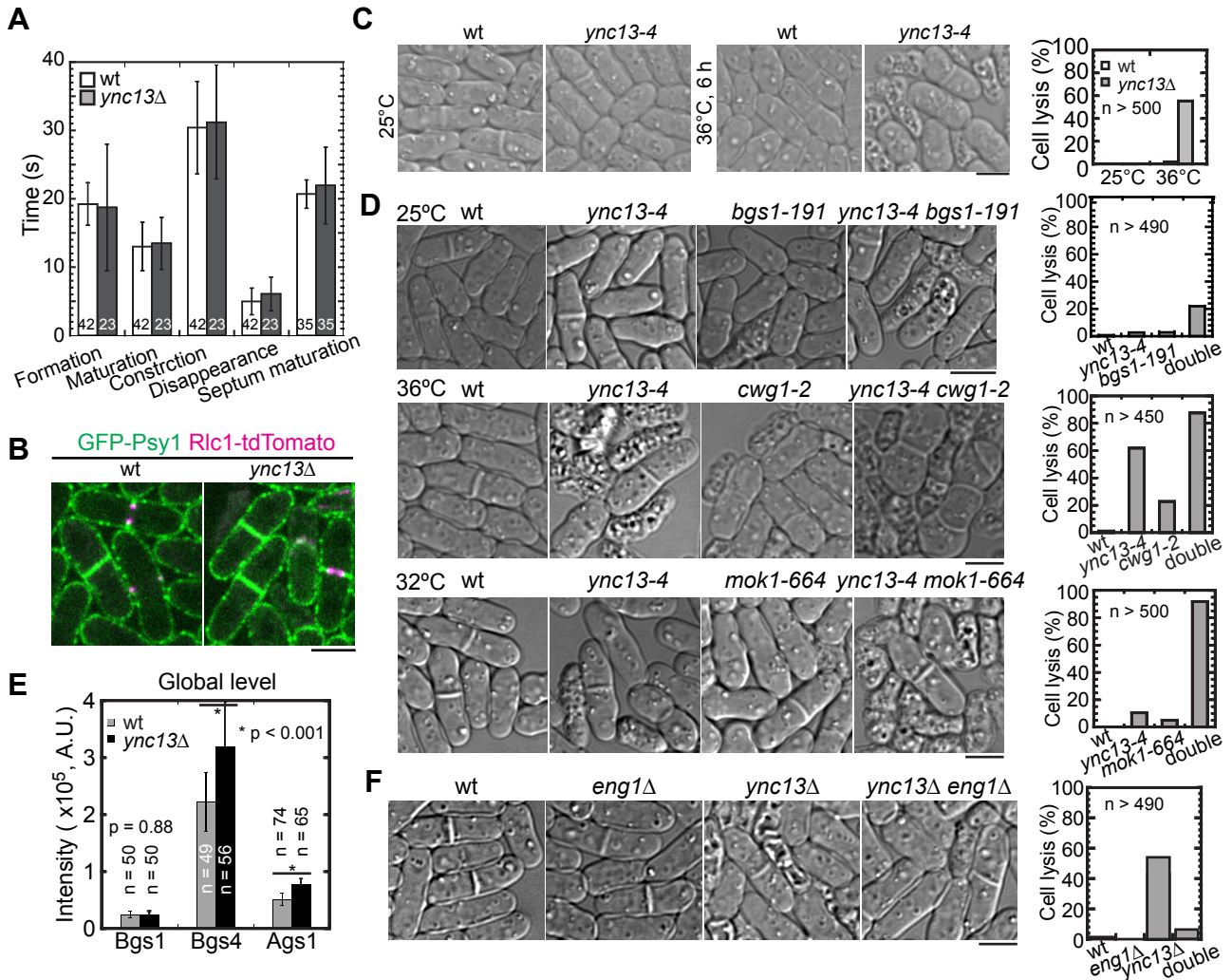


FIGURE S4: *ync13Δ* cells have no obvious defects in the contractile ring or plasma membrane closure, but have synthetic genetic interactions with mutants in cell wall synthases. (A) Duration for each stage of cytokinesis in *ync13Δ* cells. Formation, from node appearance to formation of a compact ring; Maturation, from the appearance of a compact ring to just before ring constriction; Constriction, the start of ring constriction to Rlc1 reaching highest pixel intensity as a dot; Disappearance, from the end of ring constriction to the disappearance of Rlc1 signal at the division site; Septum maturation, from end of ring constriction to just before the initiation of cell separation. (B) Plasma membrane (marked by GFP-Psy1) closure at the division site is not defective in *ync13Δ* cells. (C) DIC images and quantification of cell lysis in *ync13-4* cells at 25°C or after 6 h at 36°C. (D) DIC images and quantification of cell lysis to show synthetic interactions between *ync13-4* and *bgs1-191* (at 25°C), *cwg1-2* (4 h at 36°C), and *mok1-664* (4 h at 32°C). (E) The global protein levels of Bgs1, Bgs4, and Ags1 in wt and *ync13Δ* cells. (F) DIC images and quantification of cell lysis to show suppression of *ync13Δ* by *eng1Δ*. Bars, 5 μ m.

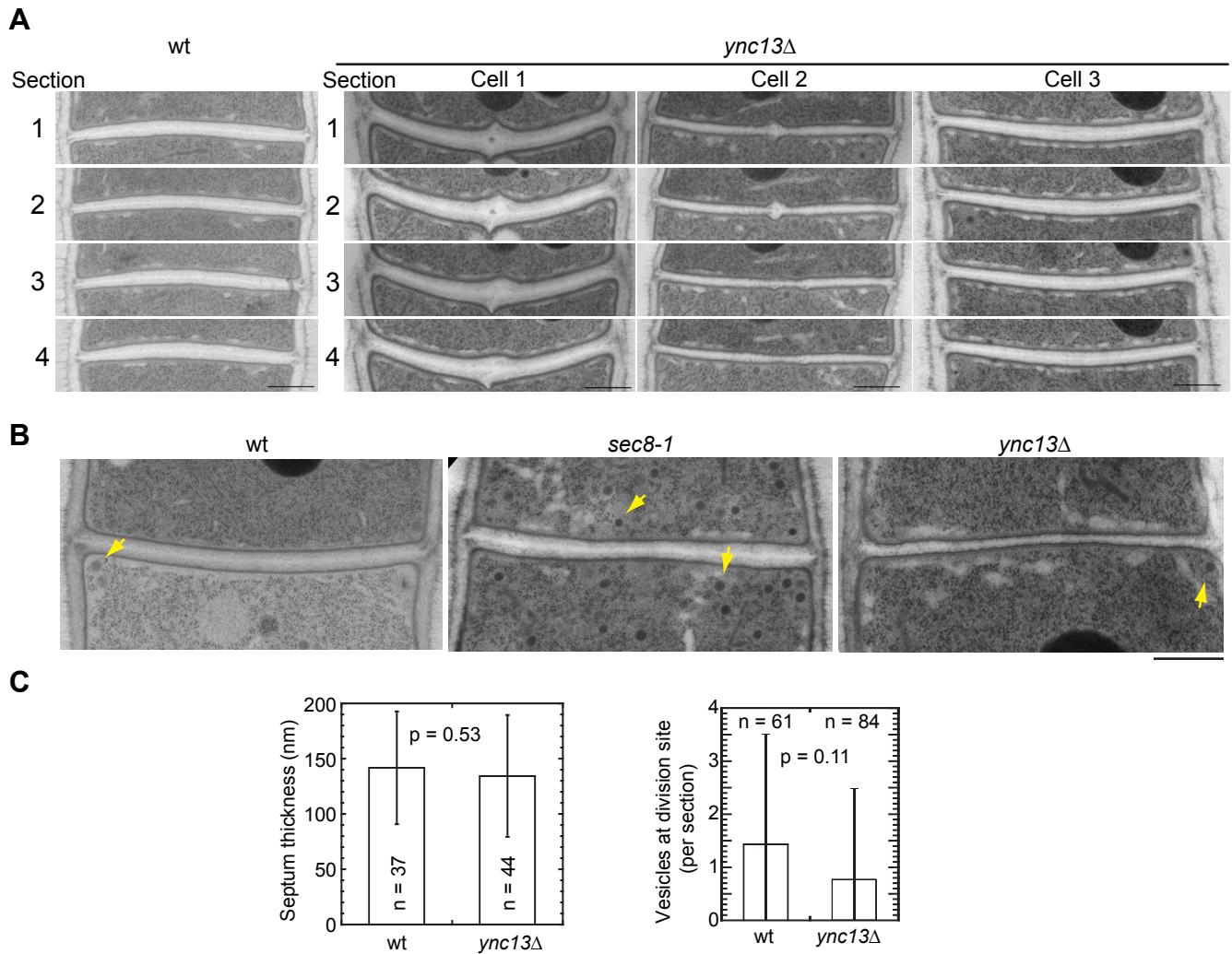


FIGURE S5: *ync13Δ* cells often have a bulge but no vesicle accumulation at the division site under EM. (A) Serial thin sections of wt (left) and *ync13Δ* cells (right). The division sites of the serial sections with 100 nm spacing are displayed from sections 1 to 4. For *ync13Δ* cells, examples of cells with a detectable bulge (cells 1 and 2) and no bulge (cell 3) are shown. (B) *ync13Δ*, unlike *sec8-1* cells, have no vesicle accumulation at the division site. The arrows mark examples of vesicles in EM images. (C) Quantification of septum thickness (left) or numbers of vesicles (right) in wt and *ync13Δ* cells. Cells with closed septa in serial thin sections were used for quantification of septum thickness. Secretory vesicles within 500 nm from the division site were quantified in each EM section. Bars, 500 nm.

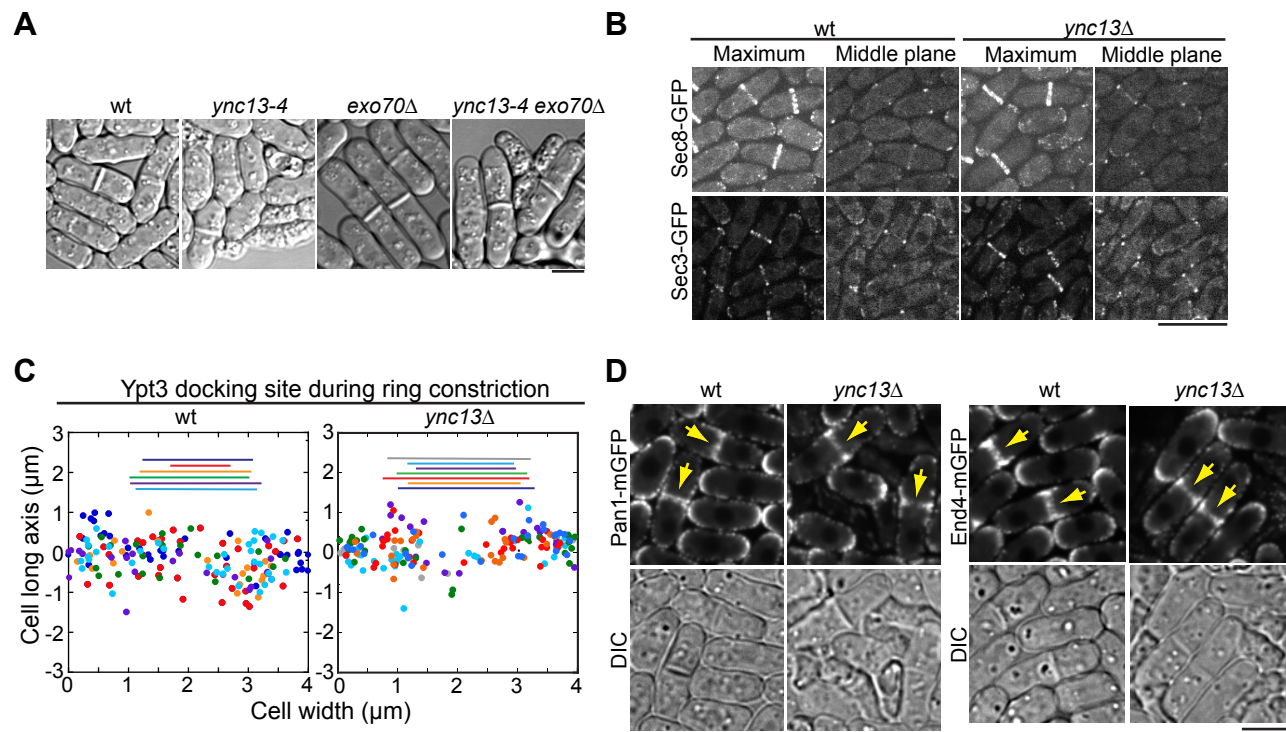


FIGURE S6: Involvement of Ync13 in exocytosis and endocytosis. (A) *ync13-4* has synthetic genetic interaction with *exo70Δ*. DIC images of cells grown at 36°C for 6 h. (B) Localization of exocyst subunits Sec8 and Sec3 is not affected by *ync13Δ*. Images of maximum projection and middle focal plane are shown. (C) Ypt3 vesicle delivery to the division site during ring constriction. The lines indicate diameters of the constricting ring for each color-coded cell. (D) Reduced localization of endocytic proteins Pan1 and End4 at the center of the division sites in *ync13Δ* cells. The sum images of 2 min continuous movies and DIC are shown. The arrows mark localization of Pan1 and End4 at the division site. Bars, 5 μm.